Phys Chem Minerals (1995) 22:351–356

PHYSICS AND CHEMISTRY OF MINERALS

Al-O^--Al Paramagnetic Defects in Kaolinite

Blandine Clozel[1,*], **Jean-Marie Gaite**[2], **Jean-Pierre Muller**[1,3]

[1] Laboratoire de Minéralogie-Cristallographie, URA CNRS 09, IPGP and Universités de Paris 6 et 7, 4, Place Jussieu, F-75252 Paris Cedex 05, France
[2] Centre de Recherche sur la Matière Divisée, U.F.R. Faculté des Sciences, Université d'Orléans, rue de Chartres, B.P. 6759, F-450567 Orléans Cedex 2, France
[3] O.R.S.T.O.M., Département T.O.A., UR12 "Geosciences de l'Environnement Tropical"

Received June 1, 1993 / Revised, accepted April 10, 1995

Abstract. Trapped holes located on Al-O-Al bonds in kaolinite were studied by electron paramagnetic resonance spectroscopy (EPR) at 9.3 and 35 GHz applied to well-crystallized, X-ray irradiated and oriented samples. The Q-band EPR spectrum is characterized by three clearly separated groups of 11 quasi-equidistant superhyperfine lines centered at $g_{xx}=2.040\pm0.0005$, $g_{yy}=2.020\pm0.0005$ and $g_{zz}=2.002\pm0.001$. In each of these groups, the 11 superhyperfine lines exhibit intensities according to the ratios 1:2:3:4:5:6:5:4:3:2:1. An angular dependence of the Q-band EPR spectrum with respect to the magnetic field is demonstrated by measurements on oriented films of kaolinite. An appropriate numerical treatment of the EPR spectra is described, which allowed extraction of the SuperHyperfine Structures (SHFS). X- and Q-band spectra have also been simulated. It is concluded from these experiments that only *one* type of center is present. This center, labelled the B-center in the literature, is very probably a hole trapped on oxygen (O^- center) atoms coupled to two octahedral aluminium.

Introduction

Various paramagnetic defects have been identified in natural kaolinite, $Al_2(Si_2O_5(OH)_4)$, by means of electron paramagnetic resonance (EPR) spectroscopy. Among these defects, are transition ions (Fe^{3+}, Mn^{2+}, VO^{2+}, Cr^{3+}) and electron or hole centers (e.g., Hall 1980; Pinnavaia 1982; Muller and Calas 1993; Gaite and Mosser 1993).

Three types of hole centers, which have been demonstrated to be radiation-induced defects (Muller et al. 1992; Allard et al. 1994), have been previously described. Two of them are O^- centers without hyperfine interaction, labelled A centers (Angel et al. 1974; Meads and Malden 1975) and A′ centers (Muller et al. 1990). These two centers produce EPR spectra showing axial symmetry. A third type of O^- centers is labelled B-centers (Angel et al. 1974). At X-band, the corresponding spectrum exhibits small modulations and is characterized by a nearly isotropic **g** factor. These modulations are interpreted as resulting from the interaction between cations each having a nuclear spin at adjacent positions. They are called SuperHyperfine Structures (SHFS). Angel et al. (1974) interpreted the B-center signal as resulting from the presence of Al in tetrahedral sites creating O^--Al_{IV} centers. Meads and Malden (1975) also suggested the presence of Al in tetrahedral sites and considered that the observed signals arose from the superimposition of signals due to O^--Al_{IV} and Al_{IV}-O^--Al_{VI} centers.

In this work, the systematic use of (i) X- and Q-band frequencies at low temperature, on powder, oriented and X-irradiated samples and (ii) a new method for signal analysis, that allows better identification of the SHFS structures, gives rise to an unequivocal assigment of B-center spectra which differs from that proposed previously.

Samples and Methods

Samples

Two reference kaolinites, both hydrothermal in origin, have been selected for this study, namely DCV and GB1. They were chosen from among the numerous kaolins originating from various environments which have been previously investigated by EPR (Muller and Calas 1993). Table 1 lists the sources, the mineralogical composition and references for the raw samples, together with main information concerning the structure and crystal chemistry of the samples used in this study. Details of the characterization of these samples can be found in Gaite et al. (1993) and Allard et al. (1994). It must be pointed out that while DCV is close to pure kaolinite, illite and quartz are present as impurities in GB1. However, it has been previously demonstrated that the contribution of illite to the EPR spectra may be neglected (Allard et al. 1994).

* *Present address:* BRGM-DR/GGP Research Division, Geotechnical Engineering and Mineral Technology, Avenue de Concyr. B.P. 6009, F-45060 Orléans Cedex 2, France
Correspondence to: B. Clozel

Table 1. Characterization of the samples: (1) deferration treatment with citrate-bicarbonate-dithionite; (2) Fourrier transform intra-red disorder index (see Muller et al. 1990); (3) structural disorder index, after Lietard 1977 (see Allard et al. 1994); (4) content of Fe(I) and Fe(II), the two trivalent iron species substituted for Al, determined according to the simplified procedure of Mestdagh et al. (1980), for 40 mg and a gain of 1000; (5) radiation-induced defects content, determined at 93 K, according to the least square decomposition of the EPR spectrum (see Allard et al. 1994)

Samples	DCV	GB1
Source	Decazeville (S.W., France)	St Austell (Cornwall, U.K.)
Environment	Hydrothermal	Hydrothermal
References	Belenguez and Revel (1986)	Cases et al. (1982)
Studied fraction	$<2\ \mu m$	total
CBD treatment[1]	yes	no
Mineralogy	Kaolinite ($\approx 100\%$)	Kaolinite ($>87\%$) Illite (5–8%) Quartz ($<5\%$)
Chemical analysis		
Major elements (wt %)		
SiO_2	46.51	46.57
Al_2O_3	39.03	37.96
Fe_2O_3	0.25	0.44
MnO	traces	traces
MgO	traces	0.08
CaO	traces	traces
Na_2O	traces	0.05
K_2O	traces	0.58
TiO_2	traces	0.04
P_2O_5	0.08	0.13
I.O.L.	14.04	13.97
Total	99.91	99.82
Radioelements (ppm)		
U	<1	7.8
Th	<1	12.2
FTIR: DIR index[2]	0.97	1.01
DRX: R2 index[3]	1.36	1.12
Coherent domain thickness	>1500 Å	500 Å
Paramagnetic centers content (a.u.)		
[Fe(I)][4]	1.5	9
[Fe(II)][4]	290	270
[RID][5] A	0.8	4.9
A′	0.4	3.4
B	0.1	3.3

EPR Experiments

Experiments were performed using Varian spectrometers. At X-band, the frequency was measured directly with a Hewlett Packard frequency meter and the magnetic field was calibrated with a NMR Gaussmeter. At Q-band, the frequency was indirectly determined from the resonant field of the DPPH standard. In both cases, the original spectrometers were modified to obtain numerical records of spectra. It has been shown (Clozel 1991) that a better resolution is obtained for the superhyperfine structures present on B-centers spectra at temperatures between 50 and 200 K. Therefore, measurements were performed at 77 and 150 K.

Oriented Samples

EPR spectra of polycrystalline samples such as kaolinite consist of the superimposition of absorption lines from each of the single micro-crystals randomly distributed throughout space. However, micro-crystals of kaolinite exhibit a platy morphology with a preferential development of layers according to the (a,b) plane. It is thus possible to obtain, either by compression or by sedimentation, an oriented film in which all (a,b) planes of kaolinite crystals are approximately parallel to each other. X-ray diffraction patterns of the resulting films, were the incident X-ray beam is perpendicular to the film, confirmed that both orientation methods were effective: the obtained patterns exhibited only 00l peaks, indicating that the common c* axis of all micro-crystals were nearly parallel.

It must be noted that the orientation procedures used do not allow for a perfect recognition of the crystallographic axes a and b which are randomly distributed in the plane of the film. However, the systematic study of the shape of the EPR spectra as a function of the angle θ measured between c* and the applied magnetic field enabled an improvement in the characterization of the defect center, with respect to the three crystallographic axes.

Characterization of the B-Center Spectra: Physical and Numerical Treatments

In the spectra of the samples studied here, the signal corresponding to the B-center is superimposed on the EPR signals caused by the A and A′ centers (Muller et al. 1992). For a better characterization of the B centers, signal enhancement was therefore required. This has been achieved by using two complementary approaches.

(1) The first approach consisted of a preliminary X-ray irradiation, which is known to create mainly centers of the B type (Angel

et al. 1974). DCV and GB1 samples were thus X-ray irradiated for 48 hours from a MoKα anti-cathode source (35 mA, 50 kV). The samples, placed in small pockets of X-ray transparent material (Milar), were set close to the shutter. After irradiation both samples exhibited stronger B center signals. However, due to the presence of strong signals from A and A′ centers, which were difficult to separate from the B center signal, GB1 was heated at 450° C for 48 hours prior to irradiation. As shown by Angel et al. (1974) and Clozel (1991), this annealing drastically reduces the concentration of all centers. Consequently, after X-irradiation of the GB1 sample the majority of centers were of type 3.

(2) The second approach utilized to enhance the B-center signal consisted of a numerical treatment of the EPR spectra. This allowed extraction of the part of the EPR spectrum chracteristic of the B center, i.e. the SHFS signal. With this aim in view, it must be recalled: (i) that the SHFS signal is a pseudo-periodic function and, (ii) that the convolution of a periodic function by a square function, whose width is equal to the period, removes the periodicity. Thus, the experimental EPR spectra were first convoluted by a normalized square function having a width equal to the hyperfine splitting. A curve without any undulations, which was comparable with the general envelope of the experimental spectrum, was obtained. The SHFS signal was thus obtained by substracting the convoluted signal from the experimental one. Such a numerical treatment allowed for detailed observation of the SHFS lines.

Results

The X-band EPR spectra obtained for the GB1 powder sample are presented in Fig. 1. In the spectra of the untreated sample (Fig. 1a and 1b), the B-center signal is masked by the resonant lines of the A- and A′-centers. Moreover, the undulations due to SHFS are visible only at low temperature (Fig. 1b). By contrast, the SHFS are clearly observed on spectra obtained after annealing and X-irradiation (Fig. 1c and 2a). The spectrum convoluted according to the procedure presented above is shown in Fig. 2b (dashed line). That obtained by substracting the convoluted signal from the experimental one is composed of nineteen, enhanced superhyperfine lines (Fig. 2c). However, a clear interpretation of this kind of spectrum cannot be achieved as it may result from the overlapping of several groups of SHFS lines. Thus, it is not possible to know whether the observed lines originate from different centers or not.

To obtain a better separation of these lines, Q-band experiments were performed. The Q-band EPR spectra of DCV and GB1 samples are presented in Fig. 3a and Fig. 3b, respectively. It is observed that the two spectra are very similar. Their general shape is characteristic of one center with an anisotropic **g** factor, $\mathbf{g}_{xx}$, $\mathbf{g}_{yy}$ and $\mathbf{g}_{zz}$ being the three eigenvalues of the **g** matrix. To perform the numerical treatment of these spectra, it was necessary to treat separately the different groups of lines since the SHFS splitting is slightly different from one group to another. The width of the square function was taken as equal to the superhyperfine splitting of each group of lines. Spectra of DCV and GB1 samples obtained after the numerical treatment were similar. That of GB1 is presented in Fig. 3c and the **g**-values and SHFS parameters are given in Table 2.

From Fig. 3c, it is clear that the SHFS on the Q-band spectra consists of three groups of 11 lines with intensities in the ratios of 1:2:3:4:5:6:5:4:3:2:1 centered on the three g_{ii} values (Table 2). This SHFS pattern is due to the interaction of a $S=1/2$ spin with two equivalent nuclei having an $I=5/2$ nuclear spin, i.e. to the presence of only one paramagnetic center.

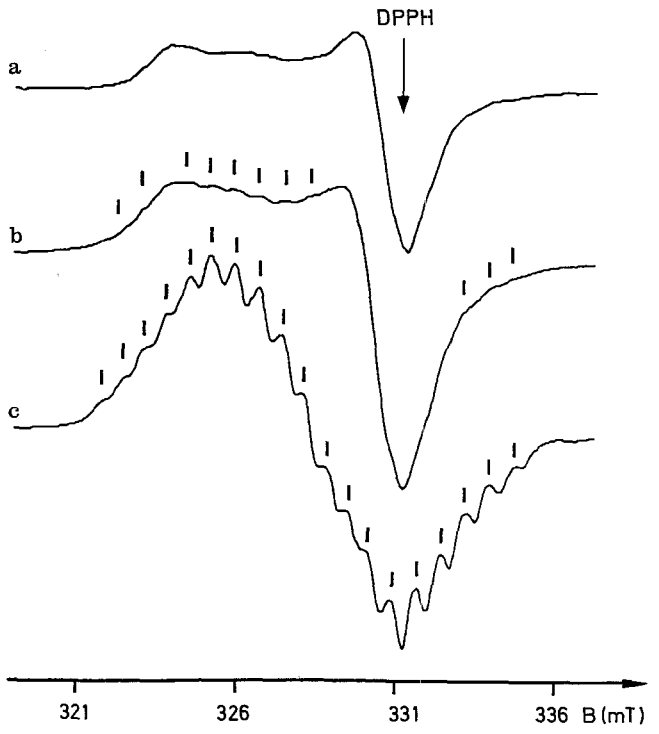

Fig. 1a–c. X-band (ν: 9.28 GHz) EPR spectra of untreated GB1 kaolinite. **a** at room temperature, showing the main asymmetric A-center signal (gain 10^3); **b** at 77 K, showing some of the superhyperfine structures due to B-centers (gain 10^3). **c** the 77 K spectrum (after annealing at 400° C for 48 hours and X-ray irradiation) of the kaolinite, showing mainly the spectrum of B-centers (gain $5 \cdot 10^2$). DPPH = standard (1,1-diphenyl-2-picrylhydrazil)

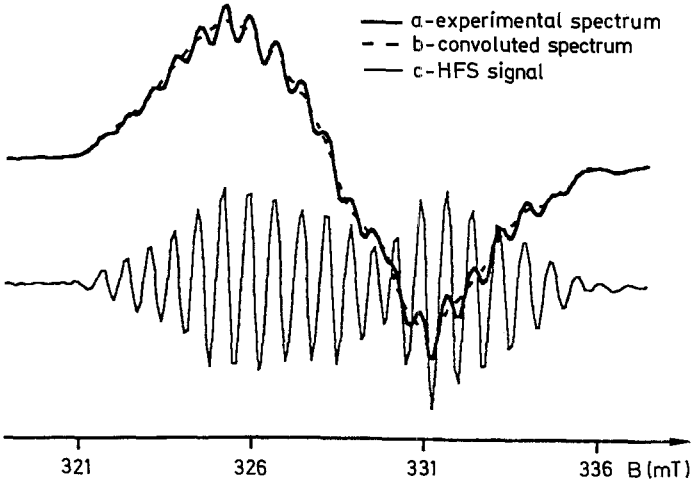

Fig. 2. X-band (ν: 9.28 GHz) EPR spectra of annealed and X-irradiated GB1 kaolinite, recorded at 150 K. Experimental spectrum; previous spectrum convoluted by a square function (convoluted signal); SHFS signal obtained after subtraction of the convoluted signal from the experimental spectrum (intensity magnified ×7)

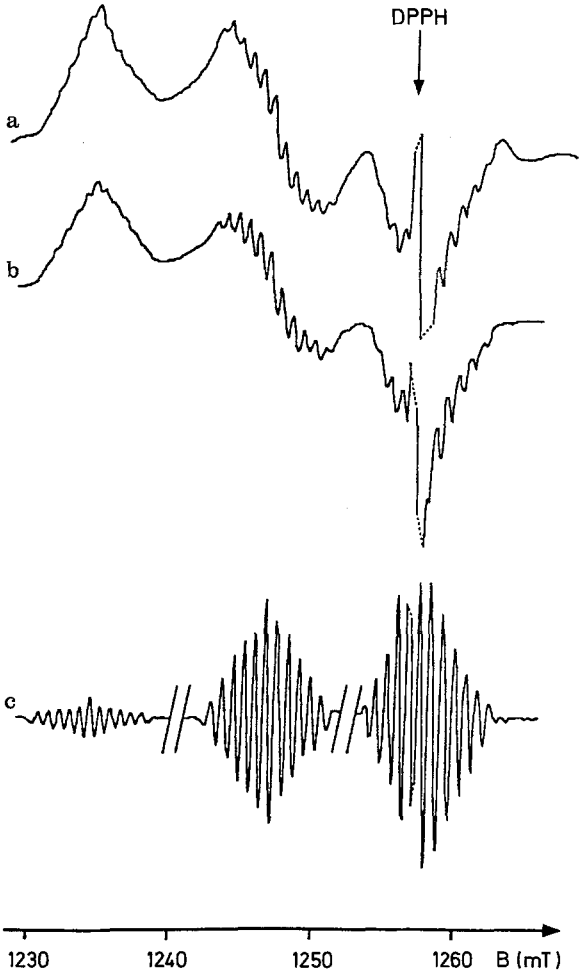

Fig. 3a–c. Q-band (ν: 35.25 GHz) EPR powder spectra of X-irradiated GB1 and DCV kaolinites, recorded at 150 K. **a** experimental signal showing well separated groups of SHFS for the DCV sample; **b** experimental signal showing well separated groups of SHFS for the GB1 sample; **c** extracted SHFS signal of the GB1 sample (with less DPPH) showing three separated groups of 11 quasi-equidistant superhyperfine lines centered at $g_{xx}=2.040\pm0.0005$, $g_{yy}=2.020\pm0.0005$ and $g_{zz}=2.002\pm0.001$, the lines from each group exhibiting intensities according to the approximate ratios 1:2:3:4:5:6:5:4:3:2:1 (intensity magnified)

Table 2. Eigenvalues of the g tensors and superhyperfine splitting values for the B-center. The values are the same for DCV and GB1 samples

g_{ii} values	g_{xx} 2.040 ±0.0005	g_{yy} 2.020 ±0.0005	g_{zz} 2.002 ±0.0005
SHFS splitting values			
in mT	0.71	0.77	0.84
in 10^{-4} cm^{-1}	6.76	7.26	7.85

The interaction of a spin S=1/2 with two equivalent nuclei of spin I=5/2 was simulated for both X and Q-band frequencies. EPR constants from Table 2 and the software from Nettar and Villafranca (1985) were used in this simulation. The simulated X- and Q-band spectra are presented in Fig. 4a and 4b. It should be noted that

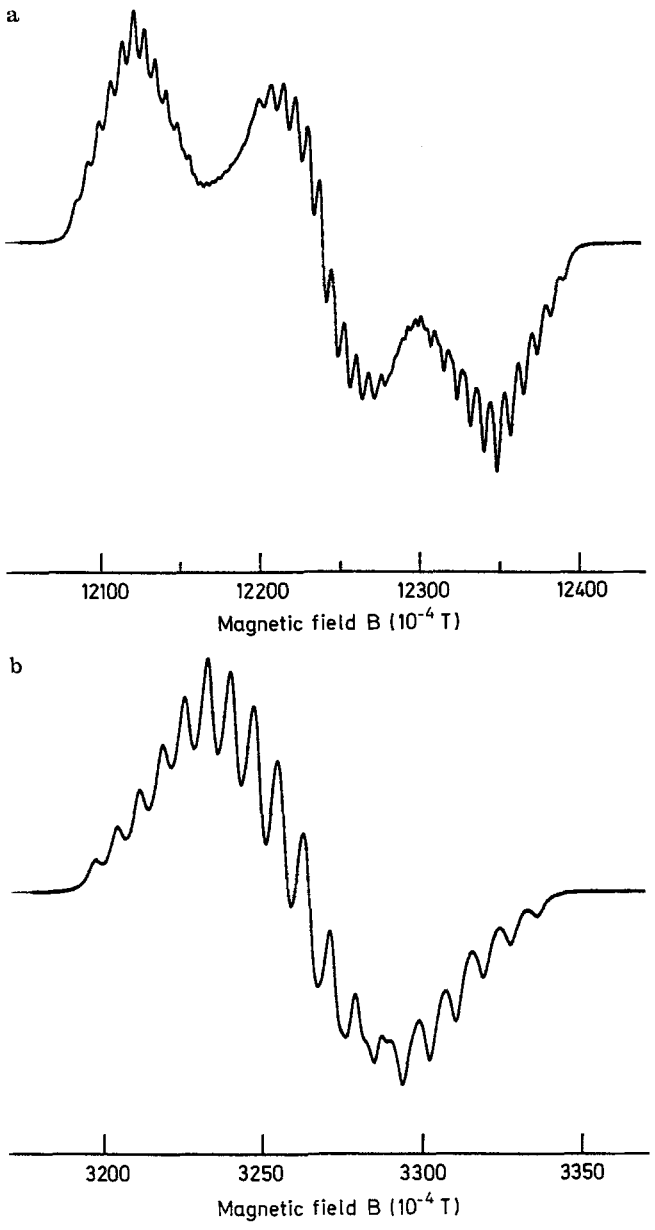

Fig. 4. Simulation of the interaction of a spin S=1/2 with two equivalent nuclei of spin I=5/2, for both Q-band (**a**) and X-band (**b**) frequencies, using EPR constants from Table 2 and the software from Nettar and Villafranca (1985)

the shape of the simulated spectra is very similar to that of the experimental spectra. This proves that the experimental spectra are due to only one type of center.

More information about the B-center has been obtained using oriented films. The orientation dependence of the B-center spectrum of the DCV sample is shown in Fig. 5 for two different orientations of the crystallites with respect to the magnetic field **B**. The relative intensities of the three groups of lines depend strongly on the orientation of the film relative to the direction of magnetic field (**B**). From a step-by-step study of the angular dependence of the intensities, it was observed that the central group (g_{yy}) reaches its maximum intensity for $\mathbf{B}\perp$(a,b) plane ($\Theta=90°$) while the low and high field

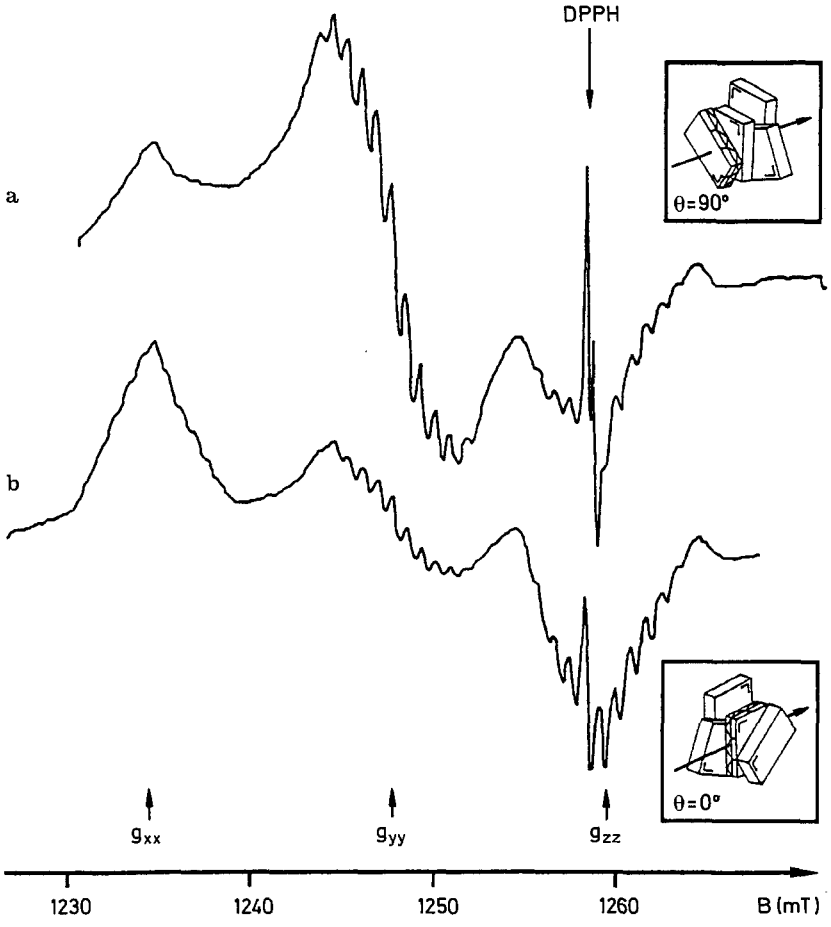

Fig. 5a, b. Q-band (ν:35.25 GHz) EPR spectra of X-irradiated DCV kaolinite, recorded at 150 K. **a** kaolinite (a, b) plane oriented perpendicular to the magnetic field ($\Theta = 90°$); **b** kaolinite (a, b) plane oriented parallel to the magnetic field ($\Theta = 0°$). Note that the group of superhyperfine lines centered at $g_{yy} = 2.020$ is the most intense when $\Theta = 90°$ ($\mathbf{B} \perp$(a,b) plane), while the other two groups, centered at $g_{xx} = 2.040$ and $g_{zz} = 2.002$, are more apparent when $\Theta = 0°$ ($\mathbf{B}$//(a,b) plane)

transitions (g_{xx} and g_{zz}) are at their maximum value for $\mathbf{B}$//(a,b) plane ($\Theta = 0°$). This angular dependence means that the EPR spectrum of the B-center has an orthorhombic symmetry, where one of the symmetry axes is perpendicular to the plane of the kaolinite layers ((a,b) plane). Similar observations were made for the GB1 sample.

Discussion

The B-center spectrum is typical of an electronic spin $S = 1/2$ interacting with two equivalent nuclei with nuclear spin $I = 5/2$ (e.g., Petrov et al. 1989). The superhyperfine interaction is thought to arise from a ^{27}Al nucleus which has a nuclear spin of 5/2 (natural abundance of ^{27}Al isotope = 100%). The mean **g** value of the B-center signal is greater than that for a free electron ($g_e = 2.0023$). This indicates that the B center is a trapped hole. It is proposed that the B-center is a hole trapped on an oxygen atom in an Al-O-Al bond and can be written as Al-O^--Al.

Aluminium in kaolinite is found in adjacent octahedral positions but it is also thought, from spectroscopic (see introduction) and thermodynamic (Merino et al. 1989) considerations, to occur in tetrahedral positions, i.e. substituted for Si in the tetrahedral sheet. Thus three different possibilities for the location of the B-center have to be considered:

(1) The first possibility is that the B center is a hole trapped on an oxygen atom bonding an Al in a normal octahedral position to an Al substituted for a Si in the tetrahedral sheet (Al_{IV}-O-Al_{VI} bonding). This situation is similar to that considered by Angel et al. 1974. In such a situation, the lengths of the Al_{IV}-O and Al_{VI}-O bonds are different: for example, the mean values, obtained from interatomic distances in Keokuk kaolinite (Bish and Von Dreele 1989), and in another well crystallized kaolinite (Hayes 1963), are 1.616 and 1.950 Å, respectively. The Al_{VI}-O bond is thus 17% longer than the Al_{IV}-O bond. As a consequence, the two different Al would have a different interaction with the O^-. This is not in accordance with the observed signal: the intensity ratios 1:2:3:4:5:6:5:4:3:2:1 indicate that both Al have the same interaction with the electronic spin. Thus, the possibility that B centers are of the Al_{IV}-O^--Al_{VI} type seems to be very doubtful.

(2) The second possibility which has to be considered is a hole trapped between two Al substituted for two adjacent Si in the tetrahedral layer (Al_{IV}-O^--Al_{IV} bonding). This hypothesis would explain the shape and intensities of the superhyperfine lines. Furthermore, the spacing between superhyperfine lines in kaolinite (0.8 mT) is similar to that observed for signals due to Al_{IV}-O^--Al_{IV} centers in some feldspars (0.7–0.9 mT; e.g. Speit and Lehmann 1982; Petrov et al. 1989 and references therein). The charge imbalance resulting from such substitution could act as a precursor for the center during

irradiation. However, according to the Lowenstein rule (Lowenstein 1954), which has recently been confirmed by means of NMR investigations of various phyllosilicates (e.g. Barron et al. 1985; Herrero et al. 1989), Al atoms substituted for Si tend to occupy sites as distant as possible, whatever the Al_{IV} content. Therefore, the probability that Al_{IV}-O^--Al_{IV} centers are present in the tetrahedral sheet would be much lower than that for O^- centers on a Al^{IV}-O^--Si bond. Hence, of the two types of signal expected, i.e. due to Al_{IV}-O and Al_{IV}-O-Al_{IV} centers, the intensity of the former would be by far the greatest. This again does not agree with the obtained results which demonstrate the presence of only one center located between two adjacent Al. The possibility that B centers are of the Al_{IV}-O^--Al_{IV} type must be ruled out.

(3) The third remaining possibility is that the B center is a hole trapped between two neighbouring Al atoms in the octahedral layer (normal position Al_{VI}-O-Al_{VI} bond). The defect created during irradiation would be induced by the occurrence of a vacancy or impurities, located in the octahedral or the tetrahedral sheet and are therefore responsible for the charge imbalance. The Al(1)-O(1), Al(2)-O(1), Al(1)-O(2) and Al(2)-O(2) calculated for the Keokuk kaolinite are as follows 1.930, 1.969, 1.965, and 1.936 Å, respectively (Bish and Von Dreele 1989). The difference in bond lengths between each of the two oxygens and their adjacent Al being less than 0.040 Å, i.e. 2% of the mean Al-O bond length, it can be considered therefore that two adjacent Al would have equivalent interactions with the electron spin from an O^- center. From all these considerations, it can be concluded that this last possibility is the most likely. However, it remains unknown if the O^- ion is at an oxygen or at an OH position.

Conclusion

A reasonable conclusion to be drawn from the aforementioned results and discussion is that there is only one type of radiation-induced defect located on Al-O-Al bonds in kaolinite. Labelled the B-center after Angel et al. (1974), it is a hole trapped on an oxygen bonding two Al in adjacent octahedral positions (Al_{VI}-O^--Al_{VI} bond). Thus, the previous spectroscopic assumptions that one or two centers located on oxygen bonding Al substituted for Si in the tetrahedral sheet to either Al in octahedral position (Al_{IV}-O^--Al_{VI} bonding) or Si (Al_{IV}-O^--Si bonding) are no longer considered valid.

Acknowledgments. We are most grateful to the French ORSTOM Institution for the support of this work (DYLAT program), and to Pr. Drs. S.S. Hafner and H. Rager from the mineralogical laboratory of Marburg University (Germany) for hospitality and facilities of the Q-band experiments.

References

Allard T, Muller J-P, Dran J-C, Ménager M-T (1994) Radiation-induced paramagnetic defects in natural kaolinites: alpha dosimetry with ion beam irradiation. Phys Chem Minerals 21:85–96

Angel BR, Jones JPE, Hall PL (1974) Electron Spin Resonance studies of doped synthetic kaolinite. I. Clay Minerals 10:247–255

Barron PF, Slade P, Frost RL (1985) Ordering of aluminium in tetrahedral sites in mixed-layer 21 phyllosilicates solid-state high resolution NMR. J Phys Chem 89:3880–3885

Bellenguez G, Revel J-C (1986) Etude préliminaire d'une bauxite latéritique stéphanienne du bassin de Decazeville (départment de l'Aveyron, France). C.R. Acad. Sci Paris 302:131–134

Bish DL, von Dreele RB (1989) Rietveld refinement of non-hydrogen atomic positions in kaolinite. Clays Clay Minerals 37:289–296

Cases J-M, Lietard O, Yvon J, Delon J-F (1982) Etude des propriétés cristallochimiques, morphologiques, superficielles de kaolinites désordonnées. Bull Minéral 42:439–455

Clozel B (1991) Les défauts paramagnétiques induits par irradiation dans les kaolinites. Approche expérimentale et implications géochimiques. PhD Dissertation, Paris 7 University, France

Gaite J-M, Mosser C (1993) Experimental and modelised EPR spectra of Cr^{3+} in kaolinite. J Phys C 5:4929–4934

Gaite J-M, Ermakoff P, Muller J-P (1993) Characterization and origin of the two Fe^{3+} EPR spectra in kaolinite. Phys Chem Minerals 20:242–247

Hall PL (1980) The application of the electron spin resonance spectroscopy to studies of clay minerals I. isomorphous substitutions and external surface properties. Clay Minerals 15:321–335

Hayes JB (1963) Kaolinite from Warsaw geodes, Keokuk region, Iowa. Iowa Acad Sci 70:261–272

Herrero CP, Sanz J, Serratosa JM (1989) The dispersion of charge deficits in the tetrahedral sheet of phyllosilicates. Analysis from ^{29}Si NMR spectra. J Phys Chem 93:4311–4315

Lietard O (1977) Contribution à l'étude des propriétés physicochimiques cristallographiques et morphologiques des kaolins. PhD Dissertation, Institut National Polytechnique de Lorraine, France

Lowenstein W (1954) The distribution of aluminium in the tetrahedra of silicates and aluminates. Am Mineral 39:92–96

Meads RE, Malden PJ (1975) Electron Spin Resonance in natural kalonites containing Fe^{3+} and other transition metal ions. Clay Minerals 10:313–345

Merino E, Harvey C, Murray HH (1989) Aqueous-chemical control of the tetrahedral-aluminium content of quartz, halloysite, and other low-temperature silicates. Clays Clay Minerals 37:135–142

Mestdagh MM, Vielvoye L, Herbillon AJ (1980) Iron in kaolinite II. The relationships between kaolinite crystallinity and iron content. Clay Minerals 15:1–14

Muller J-P, Calas G (1993) Genetic significance of paramagnetic centers in kaolinites. In: Bundy M, Murray HH, Harvey CC (eds) Kaolin Genesis and Utilization. Clay Mineralogical Soc, Bloomington, Indiana, pp 261–289

Muller J-P, Ildefonse P, Calas G (1990) Paramagnetic centers in hydrothermal kaolinite from an altered tuff in the Nopal Uranium deposit. Chihuahua, Mexico. Clays Clay Minerals 38:600–608

Muller J-P, Clozel B, Ildefonse P, Calas G (1992) Radiation-induced defects in kaolinites: indirect assessment of radionuclide migration in the geosphere. Appl Geochem, Suppl Issue n°1:205–216

Nettar D, Villafranca J (1985) A program for EPR powder spectrum simulation. J Mag Res 64:61

Petrov I, Agel A, Hafner SS (1989) Distinct defect centers at oxygen positions in albite. Am Mineral 74:1130–1141

Pinnavaia TJ (1982) Electron spin resonance studies of clay minerals. In: Fripiat JJ (ed) Advanced Techniques for Clay Minerals Analysis, Developments in Sedimentology 34. Elsevier, Amsterdam, pp 139–161

Speit B, Lehmann G (1982) Radiation defects in feldspars. Phys Chem Minerals 8:77–82